**Cell Reports, Volume *33***

## Supplemental Information

# *isoTarget*: A Genetic Method for Analyzing the Functional Diversity of Splicing Isoforms *In Vivo*

**Hao Liu, Sarah Pizzano, Ruonan Li, Wenquan Zhao, Macy W. Veling, Yujia Hu, Limin Yang, and Bing Ye**

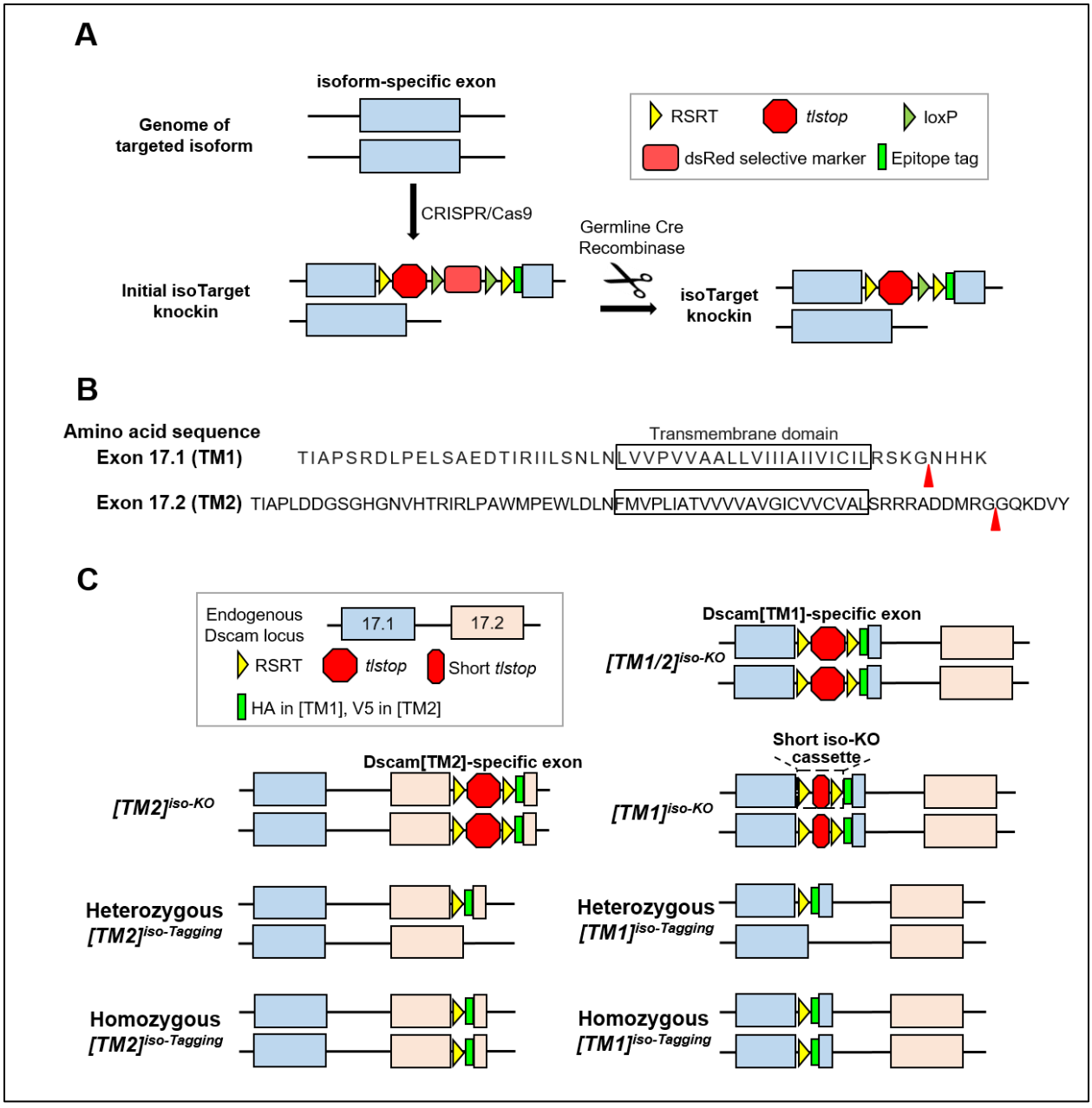


**Figure S1. The design of the *isoTarget* cassette. (Related to Figure 1)**

(**A**) At the core of the cassette is the *tlstop* box that contains multiple termination codons to ensure the disruption of mRNA translation. The *tlstop* is flanked by two RSRT sites followed by an epitope tag for achieving cell-type-specific labeling of targeted isoforms through inducible site-specific recombination. To facilitate the screening of animals with successful integrations of the *isoTarget* cassette, a transgene expressing dsRed under the 3xP3 enhancer/Hsp70 promoter is inserted in between the *tlstop* and the second

RSRT site. The dsRed transgene is flanked by two loxP sites, allowing the removal of the dsRed in the presence of Cre recombinase. The *isoTarget* cassette can be knocked into the exon encoding the targeted isoform by CRISPR/Cas9.
(**B**) The *isoTarget* insertion sites in Dscam[TM1] and [TM2] isoforms. Shown are the amino acid sequences encoded by the 17.1 (TM1) and 17.2 (TM2) exons. Red arrowheads indicate the insertion sites in the juxtamembrane regions.
(**C**) Applying *isoTarget* to study Dscam isoforms. As shown later, iso-KO of *Dscam[TM1]* impairs both *Dscam*[TM1] and [TM2] expression and is thus named *Dscam[TM1/2]*$^{iso\text{-}KO}$. We created a short *tlstop* cassette ("short iso-KO") that specifically knocks out [TM1], but not [TM2]. Iso-Tagging of Dscam[TM1] does not affect [TM1] functions. Iso-KO of [TM2] only abolishes Dscam[TM2] functions, and iso-Tagging of Dscam[TM2] does not affect [TM2] fucntions. Depending on the purpose of the experiment, Dscam[TM1] and [TM2] can be tagged either globally or specifically in targeted cell types.

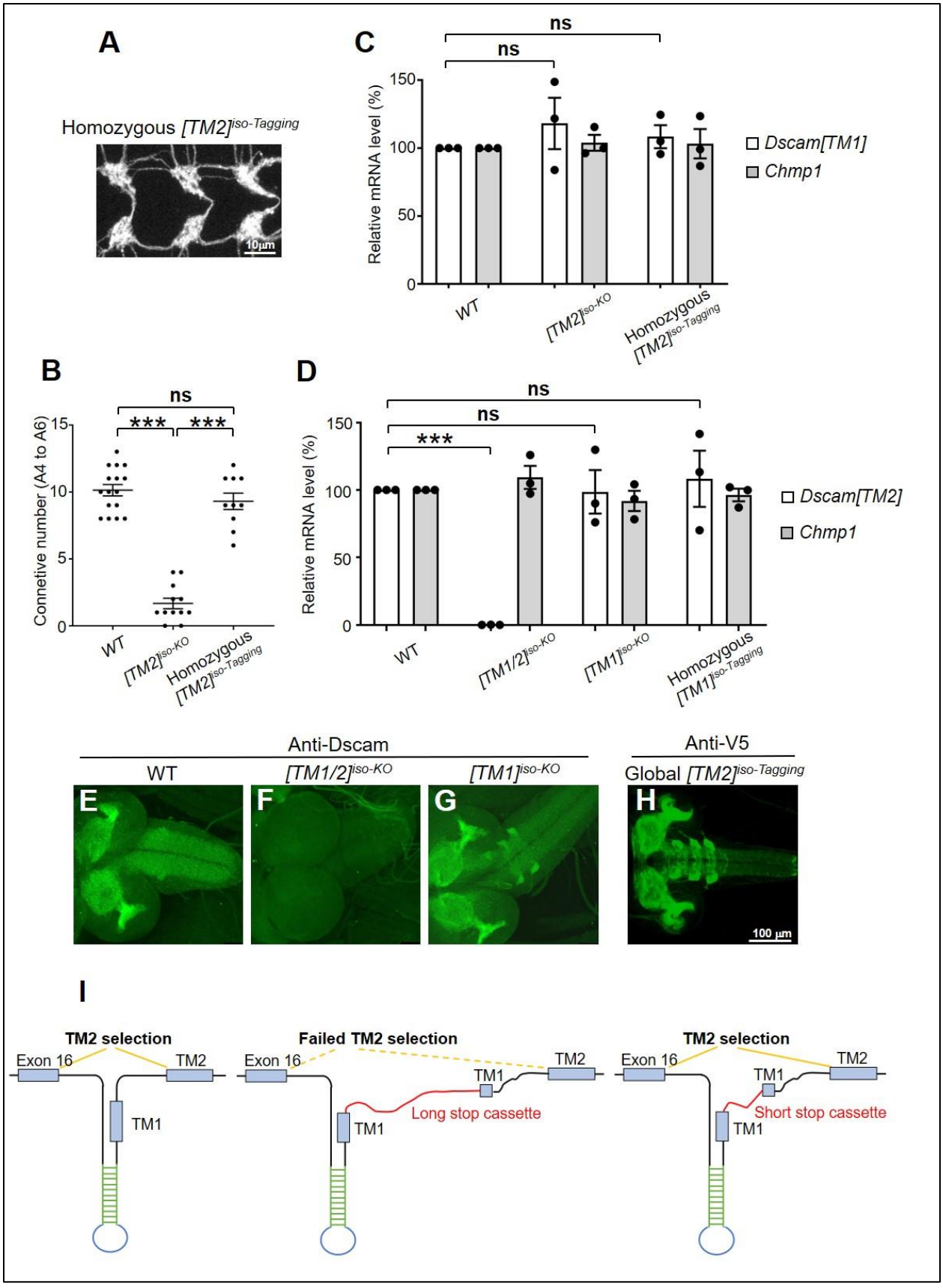
A
Homozygous [TM2]iso-Tagging
10μm
C
ns
ns
Relative mRNA level (%)
150
100
50
0
Dscam[TM1]
Chmp1
WT
[TM2]iso-KO
Homozygous [TM2]iso-Tagging
B
ns
***
***
Connetive number (A4 to A6)
15
10
5
0
WT
[TM2]iso-KO
Homozygous [TM2]iso-Tagging
D
ns
ns
***
Relative mRNA level (%)
150
100
50
0
Dscam[TM2]
Chmp1
WT
[TM1/2]iso-KO
[TM1]iso-KO
Homozygous [TM1]iso-Tagging
Anti-Dscam
Anti-V5
WT
[TM1/2]iso-KO
[TM1]iso-KO
Global [TM2]iso-Tagging
E
F
G
H
100 μm
I
TM2 selection
Exon 16
TM2
TM1
Failed TM2 selection
Exon 16
TM1
TM2
Long stop cassette
TM1
TM2 selection
Exon 16
TM1
TM2
Short stop cassette
TM1

**Figure S2. Validation of *isoTarget* and the discovery of the short *tlstop* cassette. (Related to Figure 1 and 2A-B)**

(**A**) *Dscam[TM2]*$^{iso\text{-}Tagging}$ does not affect Dscam[TM2] functions. As shown in Figure 2A and B, *[TM2]*$^{iso\text{-}KO}$ impairs axon terminal growth in C4da neurons. The axonal defect is completely rescued in homozygous global *[TM2]*$^{iso\text{-}Tagging}$ larvae generated by excision of the RSRT-tlstop-RSRT box from the iso-KO. Shown are the C4da axon terminals in A4-A6 segments.

(**B**) Quantification of the number of C4da axon connectives.

(**C**) Neither global *[TM2]*$^{iso\text{-}KO}$ nor homozygous global *[TM2]*$^{iso\text{-}Tagging}$ affect the mRNA levels of *Dscam[TM1]*. mRNAs from the whole CNS of 3$^{rd}$ instar larvae were used for reverse-transcription real-time PCR. The ΔCt value of *Dscam[TM2]* mRNA is normalized to that of the *elav* gene as descried in the Experimental Procedure. *Chmp1* serves as the internal control. Each dot represents one independent experiment.

(**D**) *Dscam[TM2]* mRNA is undetectable in global *Dscam[TM1]* isoTarget flies resulted from the insertion of the original long *tlstop* cassette (*[TM1/2]*$^{iso\text{-}KO}$), but remains intact in global *Dscam[TM1] isoTarget* flies generated by the insertion of the short *tlstop* cassette (*[TM1]*$^{iso\text{-}KO}$). *Dscam[TM2]* mRNA level is not affected in homozygous global *[TM1]*$^{iso\text{-}Tagging}$ larvae. mRNAs from the whole CNS of 3$^{rd}$ instar larvae were used for reverse-transcription real-time PCR.

(**E**-**H**) Immunostaining of the CNS with an anti-Dscam antibody shows that while Dscam expression is abolished in global *Dscam[TM1/2]*$^{iso\text{-}KO}$ (**F**), it is detectable in global *Dscam[TM1]*$^{iso\text{-}KO}$ (**G**). Moreover, the Dscam expression pattern in *Dscam[TM1]*$^{iso\text{-}KO}$ , which is presumably Dscam[TM2], is similar to endogenous Dscam[TM2] labeled by global *Dscam[TM2]*$^{iso\text{-}Tagging}$ (**H**).

(**I**) A schematic model of exon 17 selection from *Dscam* pre-mRNA, based on a previous study (Anastassiou et al., 2006). The complementary sequences (green) form a stem-loop, which is required for the selection of the TM2 exon (17.2) into *Dscam* mRNA. Inserting a long cassette into the TM1 exon (17.1) may create a long distance that eliminates the TM2 exon selection.

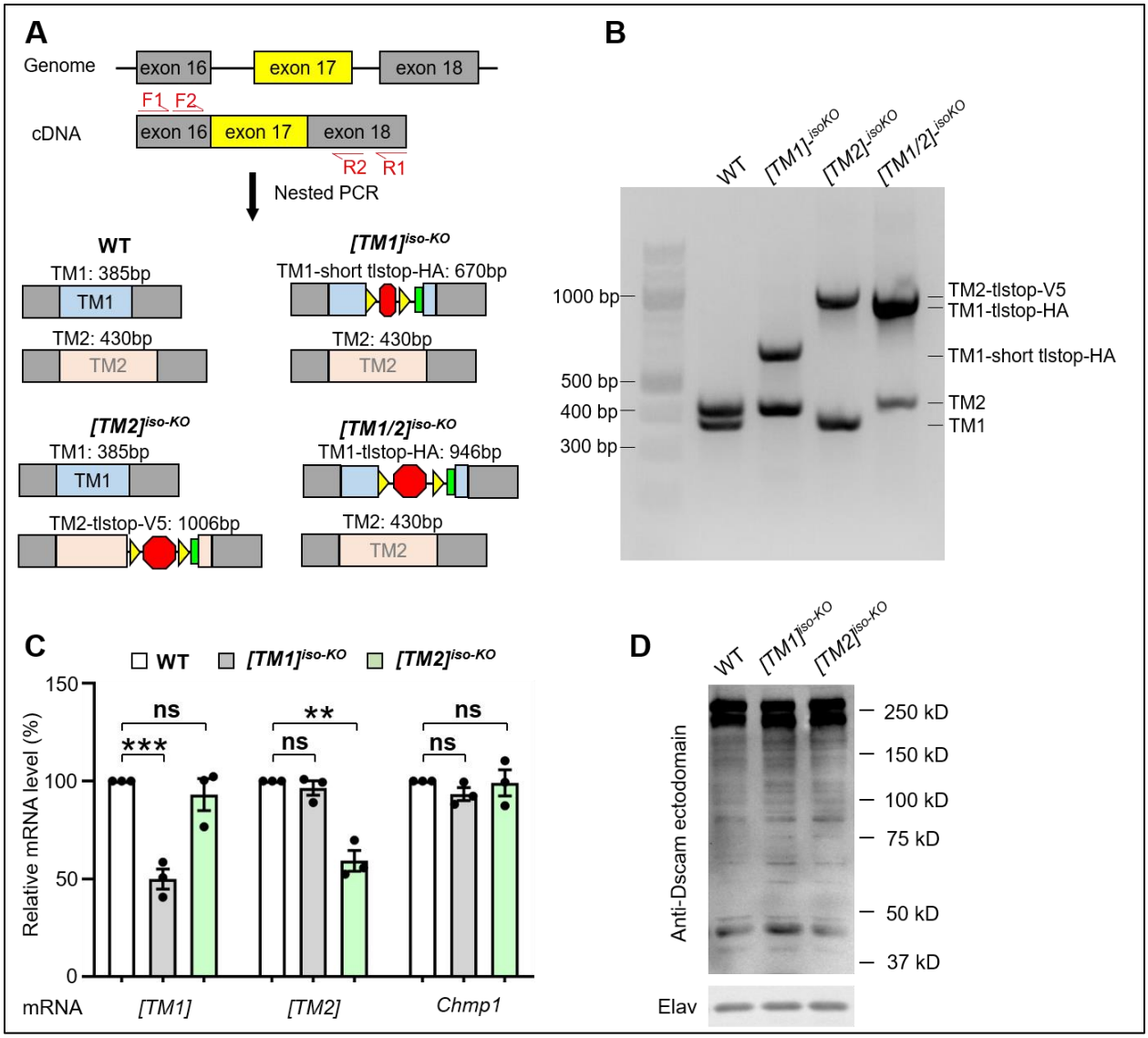


**Figure S3. The effect of *isoTarget* cassettes on alternative splicing, mRNA and protein expression of targeted isoforms. (Related to Figure 1B)**

(**A-B**) *isoTarget* cassettes do not introduce aberrant exons during alternative splicing. (**A**) Scheme of nested PCRs to detect the splicing variants between exon 16 and 18 in the *Dscam* gene in wild-type (WT), *Dscam[TM1]*$^{iso\text{-}KO}$, *Dscam[TM2]*$^{iso\text{-}KO}$, and *Dscam[TM1/2]*$^{iso\text{-}KO}$. The WT cDNAs are expected to produce the 385-bp TM1 and 430-bp TM2 bands. The *Dscam[TM1]*$^{iso\text{-}KO}$ cDNAs should produce a TM2 band (430 bp) and an altered TM1 band that contains the short iso-KO cassette (670 bp). The *Dscam[TM2]*$^{iso\text{-}KO}$ cDNAs should produce a TM1 band (385 bp) and an altered TM2

band that contains the regular iso-KO cassette (1006 bp). *Dscam[TM1/2]*$^{iso\text{-}KO}$ was used as a positive control for the assay sensitivity, as it abolishes over 99% of *Dscam[TM2]* mRNA (Figure S3A). See STAR Method for the sequences of PCR primers.

(**B**) No aberrant exon was observed in *iso-KO* mutants of *Dscam*. A dim, yet clear, 430-bp *Dscam[TM2]* band was seen in *Dscam[TM1/2]*$^{iso\text{-}KO}$, demonstrating the high sensitivity of the PCR assay.

(**C**) *isoTarget* cassettes reduce the mRNA levels of targeted isoforms. mRNAs from the whole CNS of 3$^{rd}$ instar larvae were used for reverse-transcription real-time PCR.

(**D**) Western blotting with an antibody against a common ectodomain epitope of Dscam. No band was observed at the expected size of truncated polypeptides resulting from insertion of iso-KO cassettes (~180 kD) or at other molecular weights in iso-KO mutants.

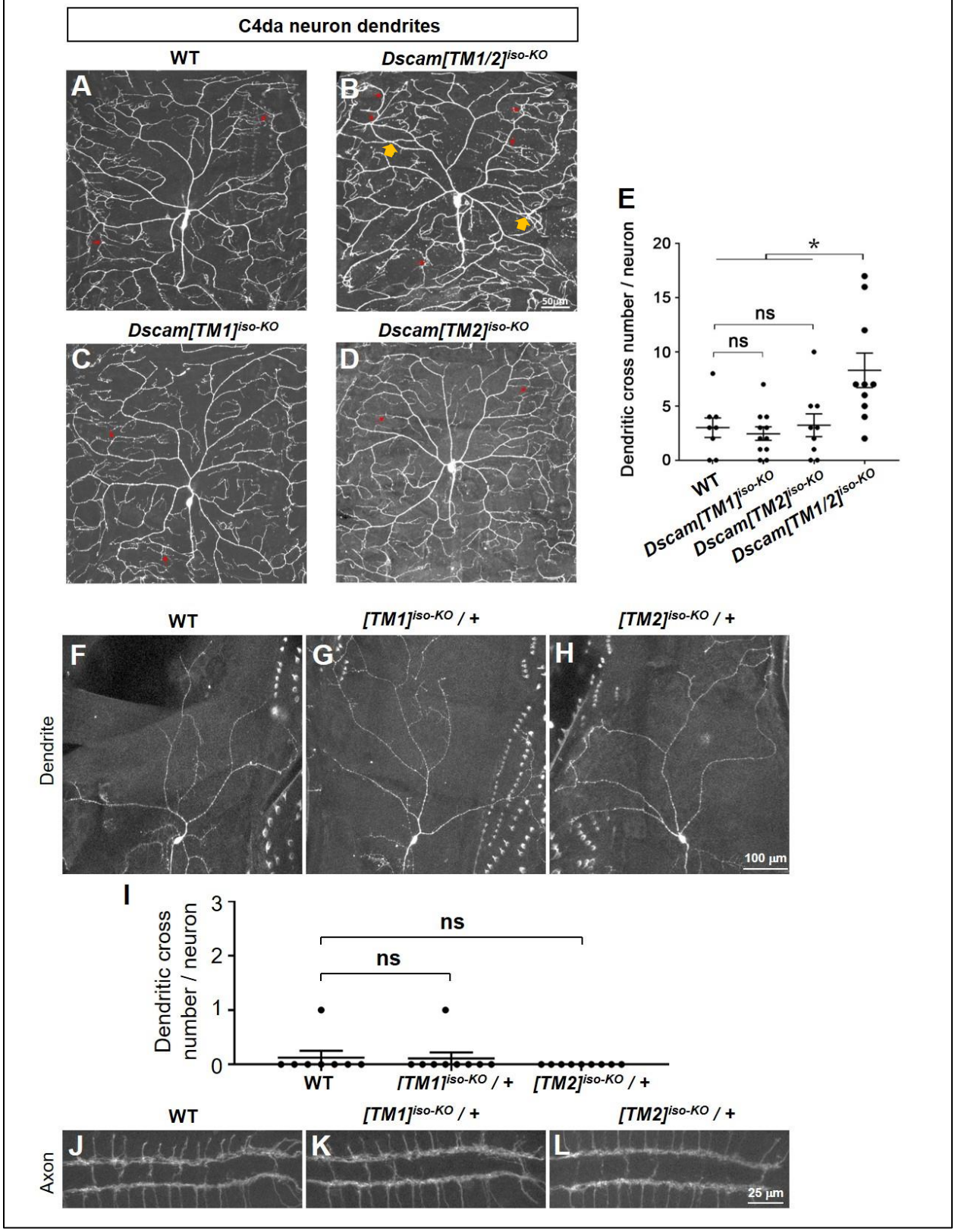
C4da neuron dendrites
WT
Dscam[TM1/2]iso-KO
A
B
50μm
Dscam[TM1]iso-KO
Dscam[TM2]iso-KO
C
D
E
Dendritic cross number / neuron
20
15
10
5
0
*
ns
ns
WT
Dscam[TM1]iso-KO
Dscam[TM2]iso-KO
Dscam[TM1/2]iso-KO
WT
[TM1]iso-KO / +
[TM2]iso-KO / +
Dendrite
F
G
H
100 μm
I
Dendritic cross number / neuron
3
2
1
0
ns
ns
WT
[TM1]iso-KO / +
[TM2]iso-KO / +
WT
[TM1]iso-KO / +
[TM2]iso-KO / +
Axon
J
K
L
25 μm

**Figure S4. *Dscam[TM1]* and *[TM2]* function redundantly in mediating dendritic self-avoidance in C4da neurons. (Related to Figure 3)**

(**A**-**D**) While *Dscam[TM1/2]*$^{iso\text{-}KO}$ (**B**) increases the crossing of dendritic branches in C4da neurons in 3$^{rd}$ instar larvae, neither *Dscam[TM1]*$^{iso\text{-}KO}$ nor *Dscam[TM2]*$^{iso\text{-}KO}$ impairs dendritic self-avoidance (**C** & **D**). Small red arrows point to crossings of fine dendritic branches, and large yellow arrows point to crossings of major dendritic branches, which is only observed when both isoforms are lost.

(**E**) Quantification of dendritic branch crosses in the C4da neuron ddaC.

(**F**-**L**) *Dscam*$^{iso\text{-}KO}$ mutants are not dominant negative. Compared with WT (**F**), no dendritic self-avoidance is observed in heterozygotes of *Dscam[TM1]*$^{iso\text{-}KO}$/+ (**G**) or *Dscam[TM2]*$^{iso\text{-}KO}$/+ (**H**). Quantification of dendritic branch crossings in the C3da neuron ddaF is shown in (**I**). Compared with WT (**J**), no axonal growth defect is observed in C3da neurons in larvae that are *Dscam[TM1]*$^{iso\text{-}KO}$/+ (**K**) or *Dscam[TM2]*$^{iso\text{-}KO}$/+ (**L**). Sample numbers (neurons) for **F-H**: WT, 8; *Dscam[TM1]*$^{iso\text{-}KO}$/+, 9; *Dscam[TM2]*$^{iso\text{-}KO}$/+, 9. Sample numbers (VNCs) for **J-L**: WT, 7; *Dscam[TM1]*$^{iso\text{-}KO}$/+, 7; *Dscam[TM2]*$^{iso\text{-}KO}$/+, 8.

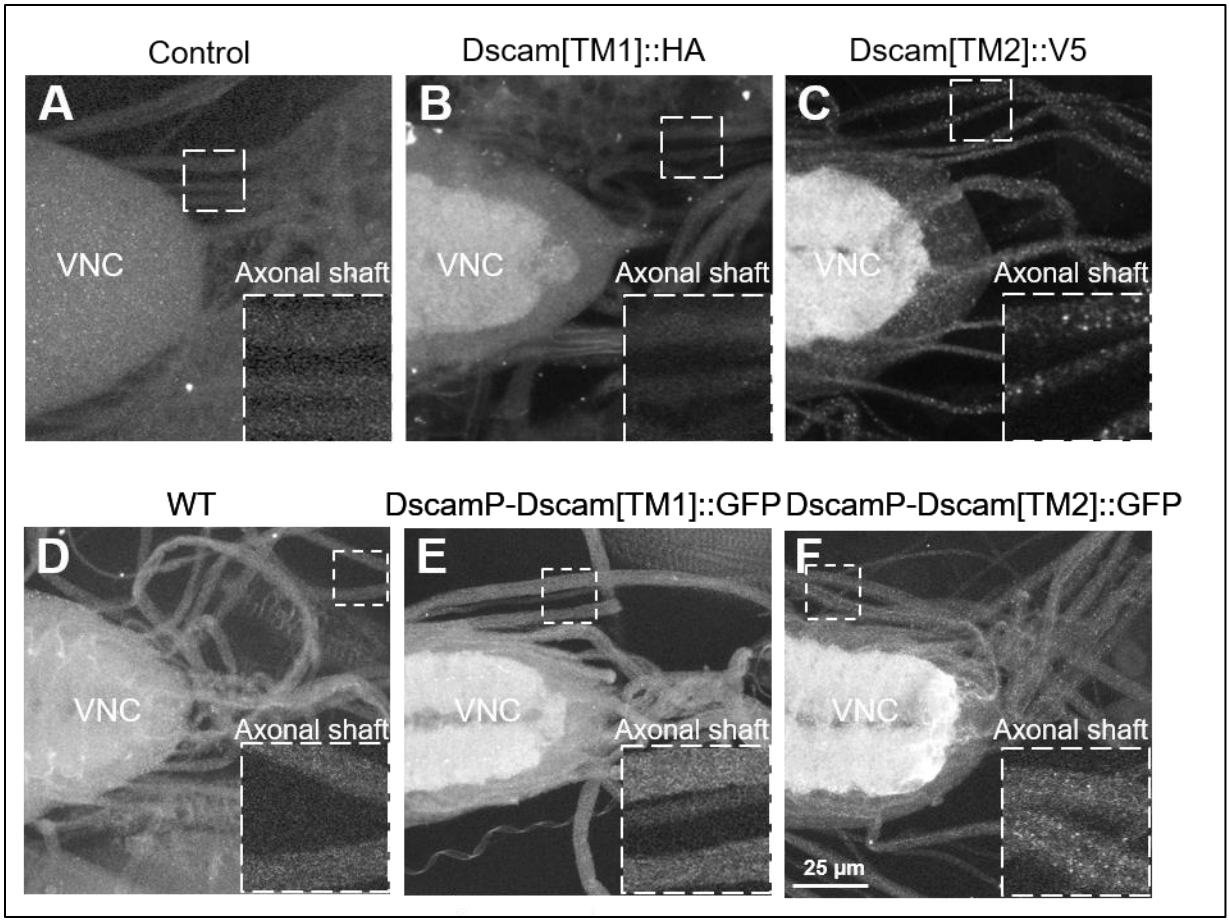


**Figure S5. Endogenous Dscam[TM2], but not [TM1], is localized in axons connecting the CNS and PNS. (related to Figure 4)**

(**A-C**) Endogenous Dscam[TM1] (Dscam[TM1]::HA$^{iso\text{-}Tagging}$) is observed in VNC neuropil region, but not in axonal shafts. By contrast, endogenous Dscam[TM2] (Dscam[TM2]::V5$^{iso\text{-}Tagging}$) is localized in axon shafts besides the VNC neuropil. The insets are magnified views of the boxed regions.

(**D-F**) Transgenic Dscam[TM1]::GFP expressed by the endogenous *Dscam* promoter is observed in VNC neuropil region, but not in axonal shafts. By contrast, puncta of transgenic Dscam[TM2]::GFP expressed by the endogenous *Dscam* promoter are localized in axon shafts besides the VNC neuropil.

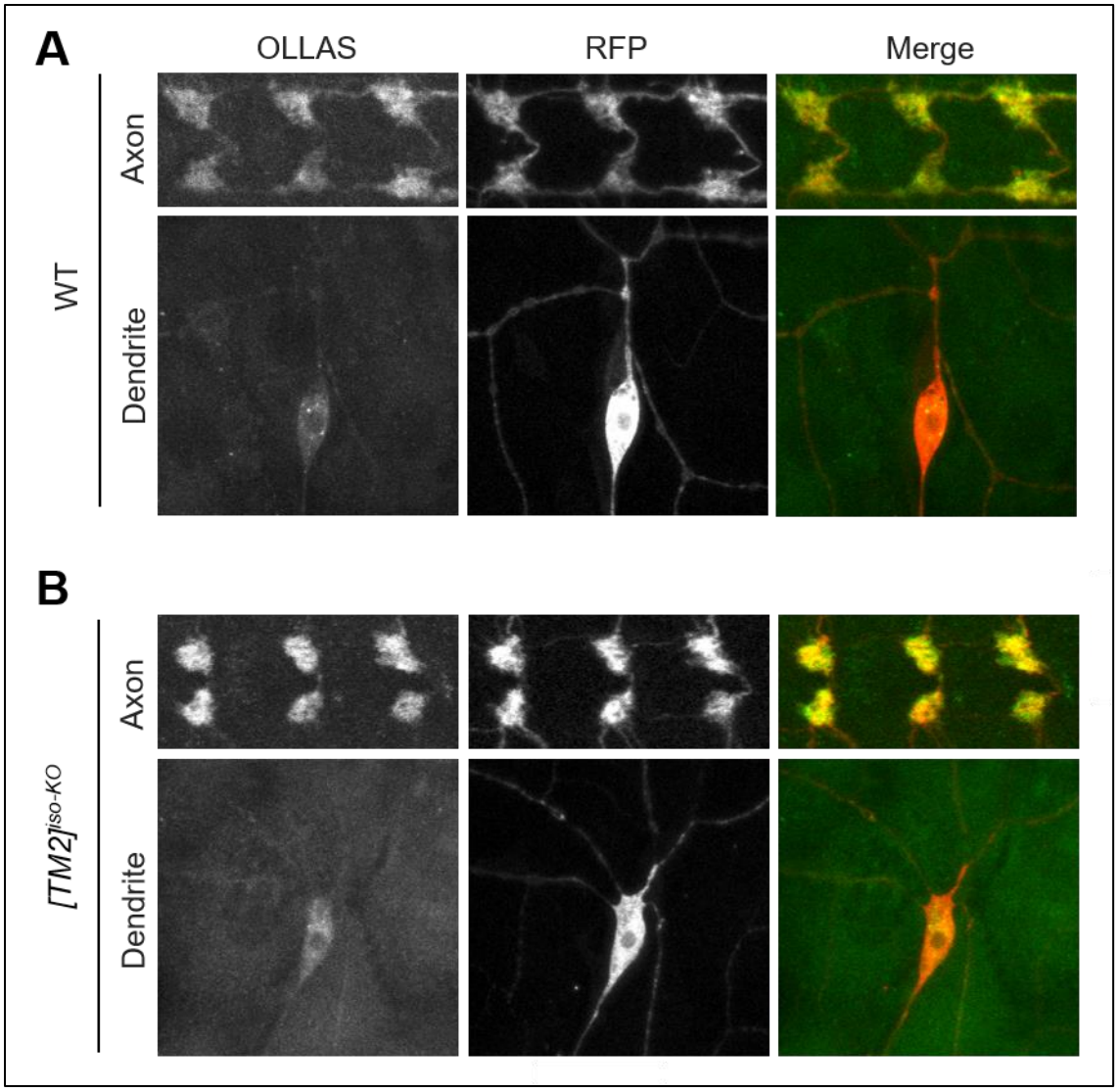


**Figure S6. Dock is enriched in axons in both wild-type and *Dscam[TM2]*$^{iso\text{-}KO}$. (related to Figure 6)**

(**A**) Dock is enriched in axons in WT C4da neurons. OLLAS-tagged Dock (Dock::OLLAS) was expressed in C4da neurons by *ppk*-Gal4. mCD8::RFP was used to label the neurons. While Dock::OLLAS is enriched in axon terminals, little is observed in dendrites.

(**B**) Dock is also enriched in axons in *Dscam[TM2]*$^{iso\text{-}KO}$

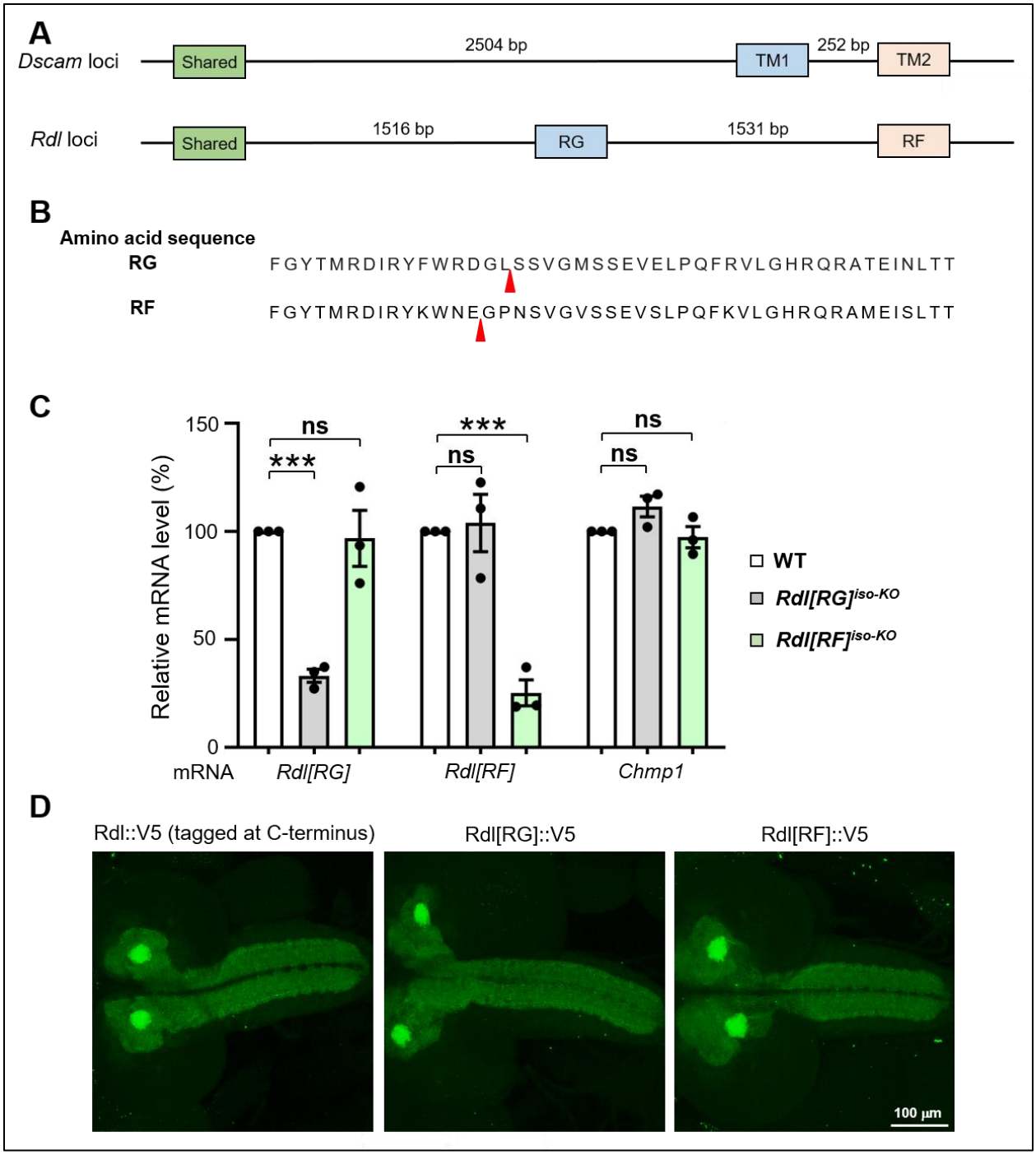


**Figure S7. Applying *isoTarget* to study Rdl isoforms. (related to Figure 1)**

(**A**) Schematics showing the introns and exons of interest in *Dscam* and *Rdl*.

(**B**) The *isoTarget* insertion sites in the RG and RF isoforms of Rdl. Shown are the amino acid sequences encoded by the RG and RF exons. Red arrowheads indicate the insertion sites.

(**C**) The full-length *iso-KO* cassette reduces the mRNA level of the targeted isoform but not that of the other isoform. mRNAs from the whole CNS of 3$^{rd}$ instar larvae were used for reverse-transcription real-time PCR.
(**D**) Endogenous RG and RF isoforms of Rdl show similar expression patterns that are comparable with that of total Rdl. The pan-neuronal driver *elav*-Gal4 was used to tag endogenous Rdl[RG] or Rdl[RF] or RDL by driving the expression of UAS-R-recombinase. Shown is the staining of V5 epitope tag.